DOI:10.5277/ABB-00476-2015-03

ZrO_2-CeO_2 ceramic powders obtained from a sol-gel process using acetylacetone as a chelating agent for potential application in prosthetic dentistry

Damian Nakonieczny[1]*, Zbigniew Paszenda[1],Sabina Drewniak[2], Tomasz Radko[3], Marcin Lis[4]

[1] Department of Biomaterials and Medical Devices Engineering, Silesian University of Technology, Zabrze, Poland

[2] Department of Optoelectronics, Silesian University of Technology, Gliwice, Poland

[3] Institute for Chemical Processing of Coal, Zabrze; Poland

[4] Institute of Non-Ferrous Metals, Division of Powders and Composite Materials, Gliwice, Poland

*Corresponding Author:

Damian Nakonieczny, Department of Biomaterials and Medical Devices Engineering, Silesian University of Technology, Roosevelta Str. 40, 41-800 Zabrze, Poland, Tel: +480322777451, e-mail: damian.nakonieczny@polsl.pl

Received: September 25th, 2015

Accepted for publication: December 12th, 2015

Abstract

Purpose: The main objective of this study was to obtain single-phase β-ZrO_2 powders with so-called '*soft agglomerates'* reproducibile morphology with acetyl-acetone as a chelating-agent. In the best of our current knowledge there is no avaiable data which determine the effect of acetyl acetone to the phase composition and morphology of ceria-doped ZrO_2 powders for biomedical appliacations.

Methods: Twenty variants of powders with different water to zirconia precursor and acetylacetone to zirconia precursor molar ratios were prepared. $0.9ZrO_20.1CeO_2$ powders were obtained by a hydrolysis and condensation and further calcination of zirconium *n*-propoxide in simply one-step sol-gel process. Influence to the phase composition of acetyloacetone to zirconia precursor ratio and water to zirconia precursor was investigated. Samples have been characterized by x-ray diffraction (XRD), Raman Spectroscopy (RS), thermal analysis (TGA/DTA) and scanning electron microscopy (SEM) measurements.

Results: Ceramic powders prepared by sol-gel process, according to the various concentration of chelating agent and water shows different morphology and phase composition.

Conclusions: Higher molar ratios of AcAc in range with smaller amounts of water cause hard agglomerates, obtained powders was characterized by very stable thermally behaviour high and various phase composition. Higher water molar ratios to zirconium-n-propoxide predispose obtaining of so-called *soft agglomerates* and one phase powders.

Keywords: Sol-Gel Process, X-ray Methods, Thermal Analysis, ZrO_2, Prosthetic Dentistry

1. Introduction

Zirconia is a type of advanced ceramic used as a thermal barrier coating in plane industry, anti-abrasive coating for cutting tools and as a functional cedramic in biomedical applications [5], [11]. Due to its mechanical strength and white color, it has been applied to dental restorations made by CAD/CAM [13],[19]. However use of zirconia in dentistry raises a lot of reservations and is associated with reports of uncontrolled phase transformation from tetragonal (β) to monoclinic (α), which occurs in oral environments [3], [16]. Results of this transformation are increases of zirconia volume and possible cracking of prostheses. Occurring changes are so-called low-temperature degradation, which especially accelerates in humid environments and with elevated temperature [2], [3], [14]. A proven route to prevent the unfavorable transformation of β-ZrO_2 is doping zirconia with metal oxides, which stabilizes the tetragonal phase in a crystal lattice and ensures the nanoscale grain size [9,10]. Currently the most commonly used dopant is Y_2O_3, which, however, does not fully ensure stability of β phase for degradation processes in human body environment [5], [11]. Based on some research results, it can be assumed that CeO_2, as a dopant, provides complete stability of the β phase and uniform grain size [5], [18],] [23]. Stabilization of β-ZrO_2 structure of cerium oxide is possible thanks to the oxygen vacancies, which further stiffen the lattice network, preventing the unfavorable phase transformation [10],[15]. Another factor that makes CeO_2 is good stabilizer of the β phase is that Ce^{4+} ion has a similar atomic radius to the Zr^{4+} ion, which additionally stiffen the zirconia crystal lattice [4].

The method of preparing of ceramic powders is also very important for stabilization. One of the best preparation methods available is the sol-gel process because it allows for strict control of the chemical composition and obtaining the homogeneous grain size distribution [6], [20], [23]. Therefore, the objective of this study is to prepare with the sol-gel method single-phase β-ZrO_2 powders doped with CeO_2 with so-called '*soft agglomerates'* reproducibile morphology effect. The phase composition of ceramic powders is an important factor for ceramic implants resistance to low-thermal-degradation in the body fluids environment fluids. Only homogeneous β-ZrO_2 ceramics is suitable for medical applications [9]. It is therefore essential that the phase composition was homogeneous as throughout all the production stages of biomedical ceramic from powders technology, green bodies preparations, compactions and solid ceramics. In the best of our current knowledge there is no information in the literature regarding the determination of the effect of acetyl acetone to the phase composition and morphology of ceria-doped ZrO_2 ceramic powders. We believe that

undertaken investigations is useful and worth for further development of zirconia ceramics for CAD/CAM systems.

2. Materials and Methods

2.1 Sample preparation

Zirconium *n*-propoxide (ZNP) (Acros Organics), 2-propanol (PrOH) (analytical grade, Avantor), acetylacetone (AcAc) (Aldrich), cerium nitrate hexahydrate (CNH) (Sigma Aldrich) and ultrapure water was used as a starting materials. All reagents were used without further purification. Whole sol-gel synthesis and reagent dosing were carried out in nitrogen in a humid-free environment. Stabilization of the zirconia precursor was achieved by the addition of acetylacetone (chelating agent). Based on previous empirical data, the molar ratio of AcAc and ZNP was fixed between 0.19 and 0.75, which obtains full-homogeneous sols and gelation times below 24 hours. The molar ratio of water and ZNP was varied between 2 and 10 with ratio change step once every two. The molar ratio of PrOH and ZNP was held constant at 2:1. The molar ratios of 20 variants of colloidal systems are presented in **Table 1**. Composition of the final powder has been calculated at 0.9 mol% ZrO_2 and 0.1 mol% CeO_2. CNH was introduced into the sealed three neck round flask as a 1 M solution in PrOH. Due to its high reactivity, water was mixed at half volume with calculated propanol and carefully added drop-by-drop as the last reagent to the sol. Obtained gels were dried at 80°C for 24 h and later grinded with mortar and pestle. Ground powders were calcined in a 2.5 h pre-heating step and appropriately at 2.5 h and 750°C. Subsequently, powders were again ground in a hand mortar. The block diagram below shows the stages of laboratory procedure (**Fig. 1.**).

Table 1 Molar ratios of prepared sols

Sample	ZNP	PrOH	H_2O	AcAc
A_1	1	2	2	0.75
A_2	1	2	4	0.75
A_3	1	2	6	0.75
A_4	1	2	8	0.75
A_5	1	2	10	0.75
A_6	1	2	2	0.58
A_7	1	2	2	0.38
A_8	1	2	2	0.19
A_9	1	2	4	0.58

A_{10}	1	2	4	0.38
A_{11}	1	2	4	0.19
A_{12}	1	2	6	0.58
A_{13}	1	2	6	0.38
A_{14}	1	2	6	0.19
A_{15}	1	2	8	0.58
A_{16}	1	2	8	0.38
A_{17}	1	2	8	0.19
A_{18}	1	2	10	0.58
A_{19}	1	2	10	0.38
A_{20}	1	2	10	0.19

2.1 Characterization

X-ray diffraction were performed on a Seifers XRD7 diffractometer equipped with Co Kα radiation (λ=0,179021 nm). The Raman spectra were taken with N-TEGRA Spectra (NT-MDT); wavelength equalled 633 nm. The TGA/DTA studies were carried out on a Q 1500D (MOM) in static air with a heating rate of 10° min^{-1} in the range from 24 to 1000°C. The morphology and level of the agglomeration was evaluated by SEM analysis. Microphotographs were taken with FEI INSPECT S50 microscope.

Fig. 1 Preparation procedure of $0.9ZrO_20.1CeO_2$ powders via controlled hydrolysis and condensation

3. Results

3.1 Synthesis

Powders obtained according to the molar ratios of AcAc and water showed differences in the structure, agglomeration and, in few cases, in phase composition. Powders where the molar ratio of water was higher than that expected from the stoichiometry were characterized by a very high degree of agglomeration. This dependence is observed for all samples in the examined range from 2 to 10, as analyzed against water: ZNP. In the systems where the water ratio was significant (from 6 to 10), the solids obtained were represented as very large "cauliflower-shaped" particles, which were very easy to grind in the mortar, resulting in smaller particles. However, a greater content of AcAc with a smaller amount of water obtained large, monolithic, crystal-like agglomerates which were hard to disintegrate with a

hand mortar. This situation particularly favors molar ratios of AcAc between 0.38 and 0.58 and the water from 2 to 4. Obtained powders based on their morphology were classified into two groups: soft agglomerates and hard agglomerates [17]. Comparative macroscopic images of soft and hard agglomerates powders after drying are shown below (**Fig. 2**).

Fig. 2 Comperative photos of: a) "hard agglomerates", b) "soft agglomerates"

3.2 Characterization

3.2.1. Thermal studies

Figure 3a–c show the samples of thermograms for extreme molar ratios of AcAc and water; for comparison, an intermediate ratios example is also given. From the TG curve it is clear that increasing concentration of AcAc lead to more shrinkage after calcination. For samples with a molar ratio of AcAc:ZNP (0.75÷0.38) and the ratio water: ZNP (2÷4), it was found that weight lost from the powders after calcination is in the range of 41.5 to 72% and corresponds to the sample shown in figure (**Fig. 3a**). For low molar ratios of AcAc: ZNP (0.19) and water from 6 to 10, weight loss was 30-35%, thermograms were similar as shown (**Fig. 3c**). Powders with an intermediate relationship of ZNP: H_2O (4 to 6) and the ZNP: AcAc (0.38÷0.58) similarly were characterized by various weight loss in the range of 37 to 48% (**Fig. 3b**). Depending on the molar ratios of ZNP: H_2O and ZNP: AcAc, it is possible to identify the characteristic peaks. On this basis, from the samples with significant differences in thermal behaviour, 3 powders samples were chosen for phase composition and SEM – morphology testing: A_1, A_3, and A_{14}. The curves from the other samples were rejected due to the lack of reproducibility and will not be taken into account in future research.

Fig. 3 Thermograms of a) A_1), b) A_3 c) A_{14}

3.2.2. X-ray diffraction

The composition and the structure of A_1, A_3, and A_{14} were confirmed by XRD analysis. **Fig. 4 a** and **b** exhibits the examples of diffraction plots of the two most differentiated powder samples: A_3 and A_{14}. The XRD pattern of A_1 was similar to A_{14} with a slightly less intensity peaks. For A_3 we found a pure monoclinic phase, the peaks at 20 = 28.49°, 32.88°, 36.70°, 40.21°, 47.71°, 52.53°, 58.95°, 59.53°, 65.31°, 78.04°. For the pure regular phase, the peaks at

20 = 35.55°, 59.60°, 71.56°. Sample (b) is full tetragonal as is A_1. For the pure tetragonal phase, peaks were 20 = 34.99°, 40.27°, 40.80°, 58.64°, 59.07°, 69.80°, 70.54°, 73.92°. A full description of the XRD-peaks are shown in **Table 2**.

Fig. 4 XRD patterns of: a) A_3, b) A_{14}

*cubic phase

Table 2 Full description of Fig. 4 X-ray patterns

A_3		
2θ(degrees)	**hkl**	**Phase**
20.279	100	Monoclinic
28.019	011	
28.484	110	
32.882	-111	
36.969	111	
41.230	200	
47.712	-211	
48.128	102	
52.526	112	
53.455	-202	
58.948	220	
63.671	300	
65.314	013	
65.630	-113	
67.546	-311	
68.454	-131	
71.121	-302	
74.453	311	
78.036	222	
35.551	111	Cubic
59.596	220	
71.556	311	
74.963	222	
A_{14}		
34.99	101	Tetragonal
40.269	002	
40.800	110	
50.096	102	

58.664	112	
59.069	200	
70.535	211	
73.915	202	

3.2.3. Raman spectroscopy

The obtained phase compositions were additionally confirmed by Raman spectroscopy. Figure (**Fig. 5 a-b.**) displays the Raman spectras for the A_3 and A_{14} samples. Five bands at 147, 268, 313, 460, and 600 cm^{-1} correspond to the Raman-active modes, which correspond to the β-ZrO_2 phase ($1A_g+2B_g+3E_g$; **Fig. 5a**.) [22]. Monoclinic zirconia shows in spectrum bands at 190, 306, 333, 475, and 638 cm^{-1} (**Fig. 5b**) [7]. In addition, there was a stated presence of cubic fluorite CeO_2 band at 465 cm^{-1}, which is a clear sign of inhomogeneity in this powder variant.

Fig. 5 Raman spectra for: a) A_{14} – full tetragonal ceria-doped zirconia, b) A_3 – monoclinic-tetragonal ceria-doped zirconia.

3.2.4. Morphology studies

Figure **(Fig. 6a-c.)** shows SEM microphotographs of samples A_1, A_{11} and A_{17}. Based on the SEM images, the difference between prepared powders with changing the molar ratios of the ZNP:AcAc:H_2O can be clearly seen. In the **Fig. 6a** a big, solid sharp-edged grains in the size in range 250-500μm is clearly shown. Additionally, there is a very low degree of grain agglomeration. Figure (**Fig.6c.**) shows the A_{17} sample with radically different morphology. A_{17} grains are significantly smaller, characterized by a considerable degree of agglomeration. From the appearance at the edge of breakthrough it can be established that they are much softer than those from sample A_1. An intermediate situation is observed for sample A_{11} (**Fig. 6b**).

Fig. 6 SEM images of the as-obtainbed poweders: a) A_1, b) A_{11}, c) A_{17}

4. Discussion

4.2. Synthesis

The well-known parameters of the sol-gel process strongly influenced the properties of the gel and final powders and especially the subsequent thermal evolution [17]. Caruso et al. [17] reported the occurrence of so-called *soft* and *hard-agglomerates*, whose shape corresponds with those obtained in our work. The binding mechanism of soft-agglomerates corresponds to

the formation of weak bonds of close-range van der Waals forces, and, therefore, the resulting powders can be easily disintegrated. On the other hand, hard agglomerate are held together by strong binding forces (chemical bonds in solid bridges) [17]. Shape and morphology of the obtained powders are very important for the preparation of green bodies and subsequent sintering of the CAD/CAM blocks. Powders from hard agglomerates require a higher pressing pressure; their structure favors inhomogeneity and the appearance of pores in green bodies. This requires raising the temperature and time of sintering, which leads to adverse changes in the phase composition of zirconia. The powders from soft-agglomerates improve sinterability, high packing density and good flowability [17].

4.2 Characterization

4.2.1. Thermal studies

For samples A_1, A_2, A_6, and A_9, TGA curves were similar (**Fig. 3a**.). Thermal decomposition was almost explosive, as can be seen from a high endothermic peak at about 233ºC, associated with the rapid decomposition of propanol, whose temeperature of decomposition was shifted due to the formation of a very stable complex between zirconia propoxide and AcAc. The big exotermic broad bump occurring in the range 248-431ºC is associated with the thermal decomposition of AcAc [12],[21]. In contrast, a very small endothermic peak in the range of 82 to 134ºC is associated with the evaporation of water.

TGA curves presented in **Fig. 3b** correspond to the curves of the samples A_3, A_4 and A_5. The presence of four characteristic peaks can be identified in the curves: the endothermic 60-110°C, associated with the evaporation of water; the exothermic at approximately. 135°C, associated with the disintegration of propanol; the exothermic at 242ºC, associated with decomposition of AcAc; and the big broad exothermic bump between 267-490°C, which we expected came from crystallization of a new phase.

The curves in **Fig. 3c** were characteristic for the powders A_{11}, A_{13}, A_{14}, A_{17}, A_{19} and A_{20}. We have identified four characteristic peaks: endothermic associated with the evaporation of water at 60-110°C; exothermic at 140°C, associated with the disintegration of of propanol; exothermic at 265°C, associated with the disintegration of AcAc; and a small sharp exothermic peak at 400°C that probably came from the crystallization of another new phase but different than it was in the case of curves shown in **Fig. 3c**.

4.2.2. Phase composition (XRD and Raman spectra)

Based on the results of XRD, we verified the presence of characteristic ”new-phase” peaks in the TGA of curves. The presence of a broad exothermic bump in the A_3 sample between 267-490ºC corresponds to the monoclinic phase (α-ZrO_2) crystallization. For A_{14} there is an occurrence of a small sharp exothermic peak at 400°C that corresponds with the crystallization of zirconia tetragonal phase (β-ZrO_2), which seems to confirm the result of XRD patterns. Referring this result to the ZNP:H_2O: AcAc molar ratios, we saw that the crystallization of the β-ZrO_2 phase favors the ratios of ZNP: AcAc in the range of 0.19-0.38 and the ZNP: H_2O in the range from 6 to 10. In contrast, crystallization of the α phase has a favorable ratio, ZNP: AcAc is equal to 0.75 and the ZNP:H_2O is from 6 to 10. Interestingly, sample A_1, has a high molar ratio of AcAc (0.75) and thus increasing the thermal stability does not caused any crystallization of α-ZrO_2 phase. Based on the data in **Table 1**, it can be stated that this situation is the result of a lower ratio of ZNP:H_2O. Also, there are no TGA curves, even at this same *new phase* peak as in the A_{14} curve, which may be explained by the "*camouflage*" by decomposing AcAc at a temperature range from 248 to 431ºC – exactly as in the crystallization temperature zone of β-ZrO_2 at 400°C. The use of Raman spectroscopy allowed to confirm results obtained by X0ray techniques

4.2.3. Morphology studies

Comparing morphology of the powders to the molar ratios, it is clear that the high ratio of ZNP: AcAc (0.75) with low water contents promotes the same formation described by Caruso et al. [19], the so-called *hard agglomerates*. However, increasing the ratio of ZNP:H_2O over 4 and decreasing the ratio of ZNP: AcAc below the 0.38 resulted in the presence of *soft agglomerates,* which may obtain full-value, doped ceria-zirconia solid green bodies. [17].

5. Conclusion

1. This work described the influence of molar ratios of chelating agent and water on a zirconia precursor as observed in phase composition and macroscopic morphology of $0.9ZrO_20.1CeO_2$ powders. It was expected that a molar ratio of AcAc and water to ZNP plays an important role in agglomerate morphology, phase composition and thermal behavior during calcination.

2. According to the obtained data, it can be stated that higher molar ratios of AcAc in range 0.58-0.75 with smaller amounts of water (2÷4) cause hard agglomerates, thermally high stable powders with various phase composition.
3. Water molar ratios higher than 6 and AcAc ratios that are reduced below 0.38 predispose obtaining of so-called *soft agglomerates* and powders with full tetragonal structure. This is particularly desirable for CAD/CAM prothetic system blocks manufacturing.
4. We hope that the obtained results allow us, in our future studies, to prepare zirconia-ceria green bodies and produce valuable blocks for CAD/CAM systems with suitable properties like poor porosity, very good compressibility and exceptionally stable mechanical properties in oral environments.

References

[1] Berendts S., Lerch M. Growth and characterization of low yttria-doped fully cubic stabilized zirconia-based single crystals, J Cryst Growth, 2013, vol. 371, 28–33.

[2] Borchers L., Stiesch M., Bach F. W., Buhl J-Ch., Hűbsch CH., Kellner T., Kohorst P., Jendras M. Influence of hydrothermal and mechanical conditions on the strength of zirconia, Acta Biomater, 2010, vol. 8, 4547–4552.

[3] Cattani-Lorente M., Scherrer S.S., Ammann P., Jobin M., Wiskott H.W.A. Low temperature degradation of a Y-TZP dental ceramic, Acta Biomater, 2011, vol. 7, 858–865.

[4] Chaim R., Basat G., Kats-Demyanets A. Effect of additives on grain growth during sintering of nanocrystalline zirconia alloys, Mater Lett, 1998, vol. 35, 245-250.

[5] Chevalier J., Gremillard L., Vikar A.V., Clarke D.R. The Tetragonal – Monoclinic Transformation in Zirconia: Lessons Learned and Future Trends, J Am Ceram Soc, 2009, vol. 92(9), 1901–1920.

[6] Colomer M.T. Straightforward synthesis of Ti-doped YSZ gels by chemical modification of the precursors alkoxides, J Sol-Gel Sci Technol, 2013, vol. 67, 135–144.

[7] Courtin E., Boy P., Piquero T., Vulliet J., Poirot N., Laberty-Robert C.A. Composite sol-gel process to prepare a YSZ electrolyte for Solid Oxide Fuel Cells, J Power Sour, 2012, vol. 206, 77–83.

[8] del Monte F., Larsen W., Mackenzie J. D. Stabilization of tetragonal ZrO_2 in ZrO_2-SiO_2 binary oxides, J Am Ceram Soc, 2000, vol. 83(3), 628–634.

[9] EN ISO 13356:2013, Implants for surgery. Ceramic materials based on yttria-stabilized tetragonal zirconia (Y-TZP).

[10] Fábregas O., Fuentes R.O., Lamas D. G., Fernández de Rapp M.E., de Reca N.W., Fantini M.C.A., Craievich A.F., Prado A.F., Millen R.P., Temperini M.L.A. Local structure of metal-oxygen bond in compositionally homogeneous, nanocrystalline zirconia-ceria solid solutions synthesized by a gel-combustion process, J Phys Condens Matter, 2006, vol. 18, 7863-7881.

[11] Hannink R.H.J. Kelly P.M., Muddle B.C. Transformation toughening in zirconia ceramics, J Am Ceram Soc, 2000, vol. 83(3), 461–487.

[12] Huang W., Yang J., Wang Ch., Zou B., Meng X., Wang Y., Cao X., Wang Z. Effects of Zr/Ce molar ratio and water content on thermal stability and structure of ZrO_2-CeO_2 mixed oxide prepared via sol-gel process, Mater Res Bull, 2012, vol. 47, 2349–2356.

[13] Kelly J.R., Denry I. Stabilized zirconia as a structural ceramic: An overview, Dent Mater, 2008, vol. 24, 289–298.

[14] Keuper M., Berthold Ch., Nickel K.G. Long-time aging 3 mol.% yttria-stabilized tetragonal zirconia polycrystals at human body temperature, Acta Biomater, 2014, vol. 10, 951–959.

[15] Lebrun N., Perrot P. Cerium-Oxygen-Zirconium, in Refractory metal systems: phase diagrams, crystallographic and thermodynamic data, Materials Science International Services GmbH, Stuttgart, 2010, 87-110.

[16] Lughi Y., Sergo V. Low temperature degradation-aging-of zirconia: A critical review of the relevant aspects in dentistry, Dent. Mater., 2010, vol. 26, 807–820.

[17] Mamana N., Díaz-Parralejo A., Ortiz A.L., Sánchez-Bajo F., Caruso R. Influence of synthesis process on the features of Y_2O_3-stabilized ZrO_2 powders obtained by the sol-gel method, Ceram Int, 2014, vol. 40, 6421–6426.

[18] Menvie Bekale V., Legros , Haut C., Sattonnay G., Huntz A.M. Processing and microstructure characterization of ceria-doped yttria-stabilized zirconia powder and ceramics, Solid State Ionics, 2006, vol. 177, 3339-3347.

[19] Miyazaki T., Hotta Y. CAD/CAM systems available for the fabrication of crown and bridge restorations, Aust Dent J, 2011, vol. 56(1), 97–106.

[20] Nakonieczny D., Walke W., Majewska J., Paszenda Z. Characterization of magnesia-doped yttria-stabilized zirconia powders for dental technology applications, Acta Bioeng Biomech, 2014, vol. 13(4), 99-106.

[21] Naumenko A., Gnatiuk I., Smirnova N., Eremenko A. Characterization of sol-gel derived TiO_2/ZrO_2 films and powders by Raman spectroscopy, T Sol Films, 2012, vol. 520, 4541–4546.

[22] Navio J.A., Marchena F.J., Macias M., Sanchez-Soto P.J., Pichat P. Formation of zirconium titanate powder from a sol gel prepared reactive precursor, J Mater Sci, 1992, vol. 27, 2463–2467.

[23] Trusova E.A., Khrushcheva A.A., Vokhmintcec K.V. Sol-gel synthesis and phase composition of ultrafine ceria-doped zirconia powders for functional ceramics, J Eur Ceram Soc, 2012, vol. 32, 1977–1981.

Figure Captions

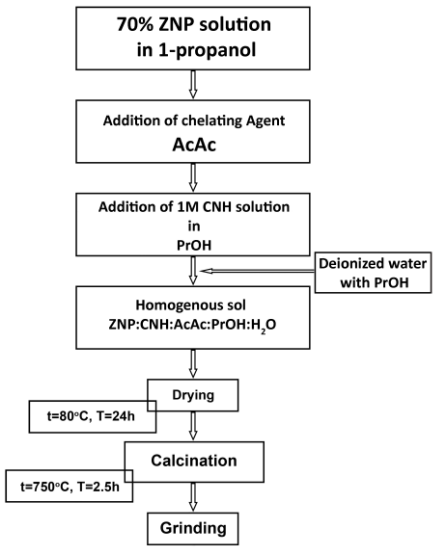

Fig. 1 Preparation procedure of $0.9ZrO_20.1CeO_2$ powders via controlled hydrolysis and condensation

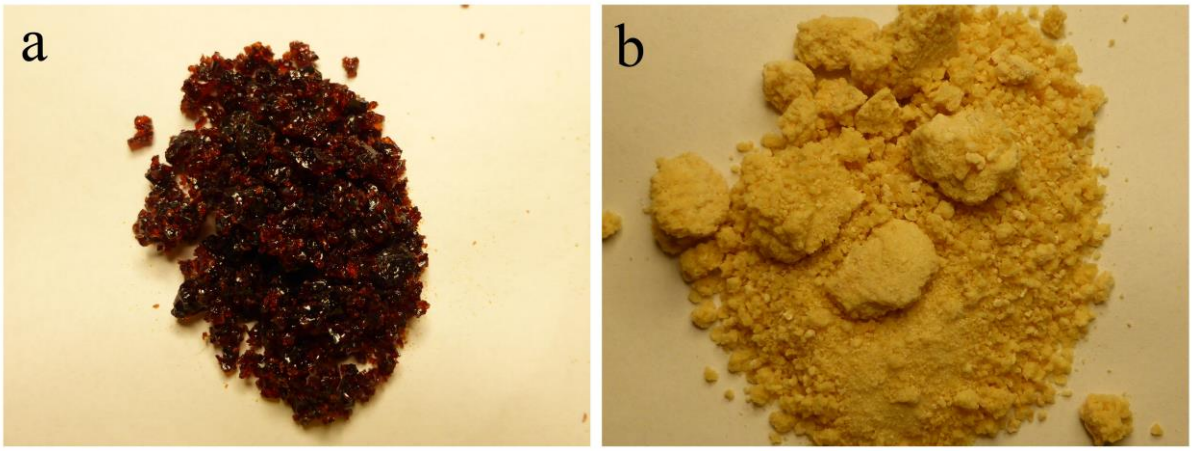

Fig. 2 Comperative photos of: a) “hard agglomerates”, b) “soft agglomerates”

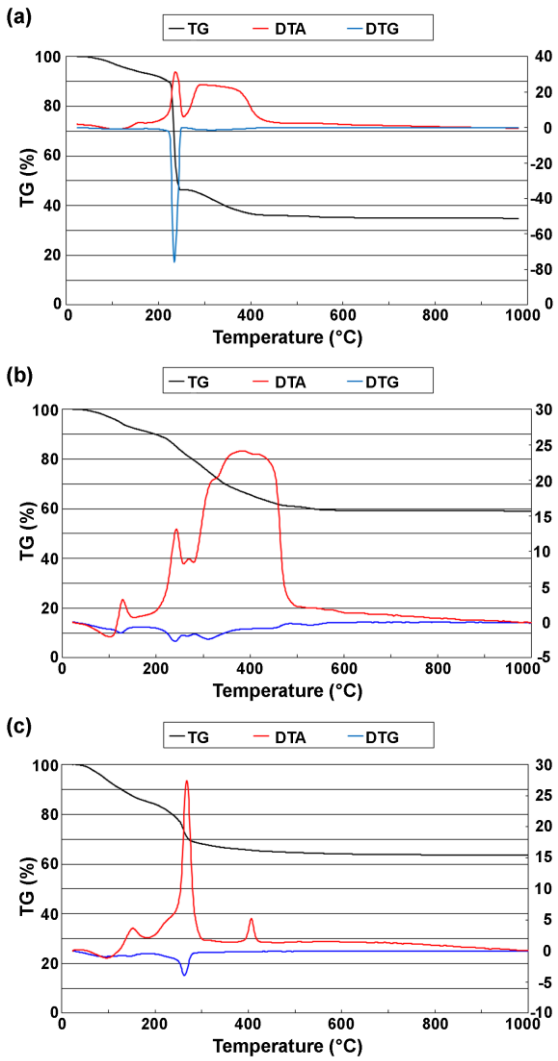

Fig. 3 Thermograms of a) A_1), b) A_3 c) A_{14}

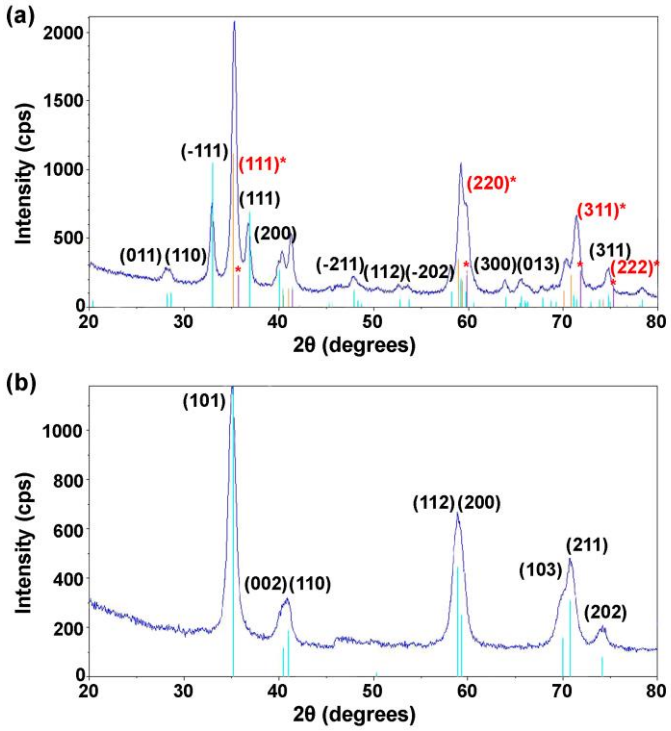

Fig. 4 XRD patterns of: a) A_3, b) A_{14}

*cubic phase

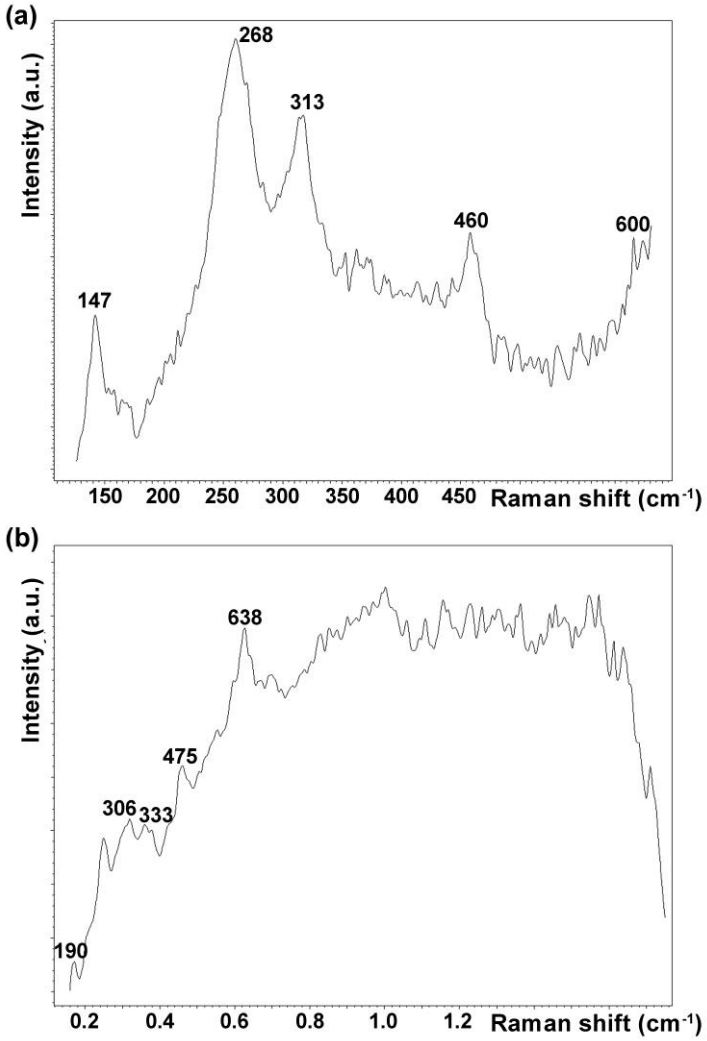

Fig. 5 Raman spectra for: a) A_{14} – full tetragonal ceria-doped zirconia, b) A_3 – monoclinic-tetragonal ceria-doped zirconia.

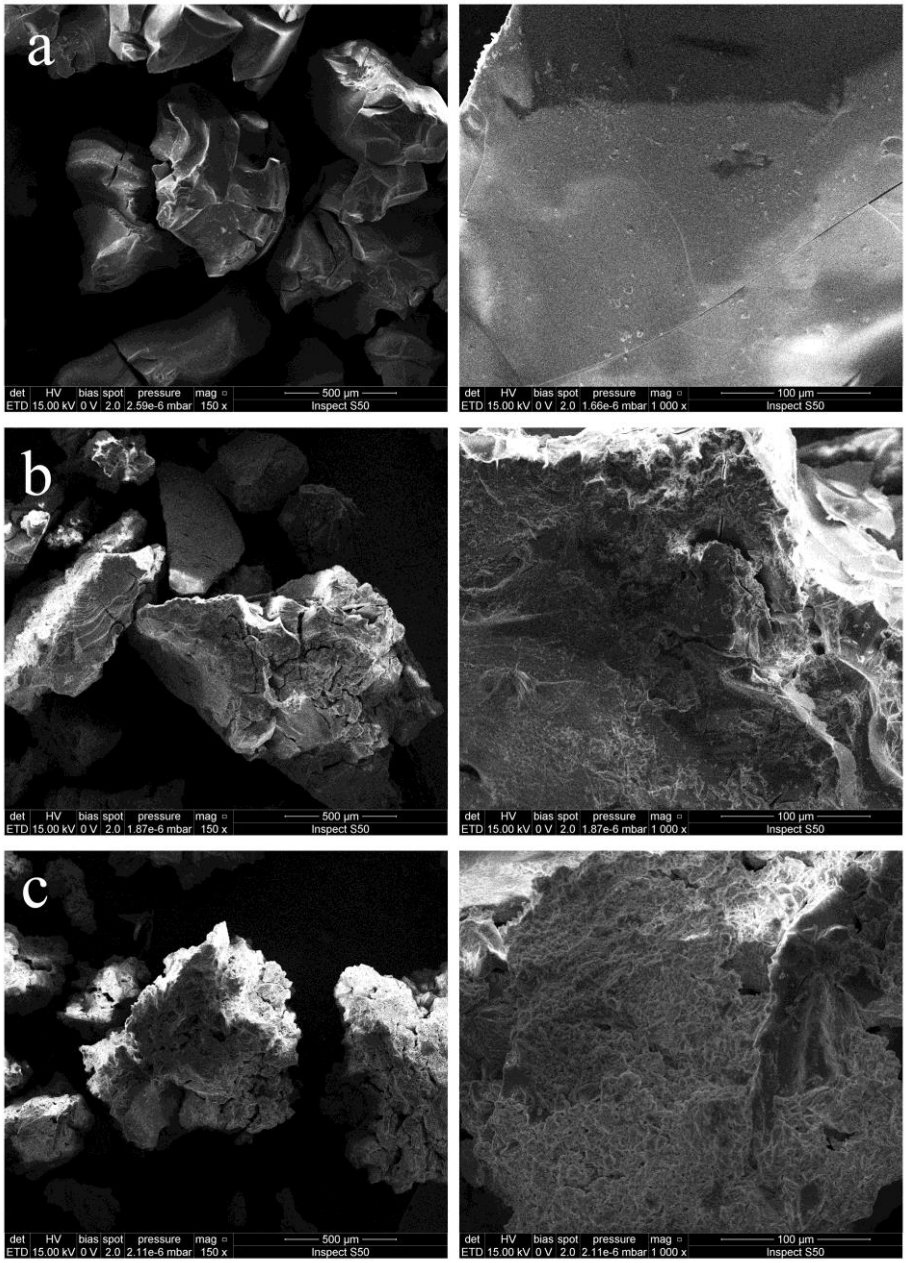

Fig. 6 SEM images of the as-obtainbed poweders: a) A_1, b) A_{11}, c) A_{17}